arXiv:cond-mat/0412197v1 [cond-mat.mtrl-sci] 8 Dec 2004

Nanoscopic Study of the Ion Dynamics in a $LiAlSiO_4$ Glass Ceramic by means of Electrostatic Force Spectroscopy

Bernhard Roling[1], André Schirmeisen[2], Hartmut Bracht[3], Ahmet Taskiran[2], Harald Fuchs[2], Sevi Murugavel[1], Frank Natrup[3]
[1] *Institut für Physikalische Chemie and Center for Nanotechnology (CeNTech), Westfälische Wilhelms–Universität Münster, Corrensstr. 30, 48149 Münster, Germany*
[2] *Physikalisches Institut and CeNTech, Westfälische Wilhelms-Universität Münster, Wilhelm-Klemm-Str. 10, 48149 Münster, Germany*
[3] *Institut für Materialphysik and CeNTech, Westfälische Wilhelms-Universität Münster, Wilhelm-Klemm-Str. 10, 48149 Münster, Germany*

(Dated: December 25, 2021)

We use time-domain electrostatic force spectroscopy (TD-EFS) for characterising the dynamics of mobile ions in a partially crystallised $LiAlSiO_4$ glass ceramic, and we compare the results of the TD-EFS measurements to macroscopic electrical conductivity measurements. While the macroscopic conductivity spectra are determined by a single dynamic process with an activation energy of 0.72 eV, the TD-EFS measurements provide information about two distinct relaxation processes with different activation energies. Our results indicate that the faster process is due to ionic movements in the glassy phase and at the glass-crystal interfaces, while the slower process is caused by ionic movements in the crystallites. The spatially varying electrical relaxation strengths of the fast and of the slow process provide information about the nano- and mesoscale structure of the glass ceramic.

1. Introduction

Glass ceramics are important materials for a wide variety of applications. Examples are low-expansion glass ceramics for cook top panels and for telescope mirrors [1, 2], thin glass ceramic films for microelectronics [3] and bioactive/biocompatible glass ceramics for bone regeneration and dental applications [4, 5].

Low-expansion glass ceramics are based on the system Li_2O – Al_2O_3 – SiO_2. The low thermal expansion coefficients arise from the negative thermal expansion coefficient of crystallites being dispersed in a glassy matrix with a positive thermal expansion coefficient. Furthermore, these glass ceramics are lithium ion conductors with a conductivity depending strongly on the degree of crystallinity. Some of the present authors have studied the lithium ion conductivity of $LiAlSiO_4$ glass ceramics with different degrees of crystallinity χ [6]. They found that starting from a $LiAlSiO_4$ glass, partial crystallisation leads to an enhancement of the ionic conductivity. This effect was attributed to fast ion conduction at the interfaces between crystallites and glassy phase. However, when χ exceeds about 40%, the ionic conductivity drops strongly with increasing χ, and the conductivity of the completely crystallised ceramic is about three orders magnitude lower than that of the glass. This suggests that the sharp drop of the lithium ion conductivity at $\chi > 0.4$ is caused by a blocking of the lithium ions by the poorly conducting crystallites.

Similar effects have been observed in composite electrolytes where insulating nanoparticles are dispersed in crystalline or polymeric ion conductors [7, 8, 9, 10]. At low volume fractions of the insulating nanoparticles, the ionic conductivity increases with increasing volume fraction, while above a critical volume fraction, the conductivity drops with increasing volume fraction. This strong composition dependence of the ionic conductivity is of interest for technical applications, since the effect can be used to prepare optimized electrolytes. From a theoretical point of view, the mechanisms of ionic conduction in such composite materials are not well understood. In the case of defect crystals with dispersed insulator particles, enhanced defect concentrations close to the interfaces between ionic conductor and insulator particles due to space charge effects are believed to play an important role [11]. However, in structurally disordered materials, such as glasses and polymer electrolytes, the high number density of mobile ions implies small Debye lengths, and therefore, it seems unlikely that space charge effects are important for ion transport. An alternative assumption is an enhanced mobility of ions close to the conductor–insulator interfaces.

A limiting factor hindering a better theoretical understanding is the traditional characterization of the ion dynamics by means of macroscopic techniques, such as conductivity spectroscopy and NMR relaxation techniques. These techniques average generally over the ion dynamics in different phases and at interfaces leading to a loss of information about the microscopic and nanoscopic mechanisms of the ion transport. Therefore, it would be desirable to develop experimental techniques which provide *spatially resolved* dynamic information.

In a recent publication [12] we have shown that time-domain electrostatic force spectroscopy (TD-EFS) using an atomic force microscope is capable of probing ion dynamics and ion transport in nanoscopic subvolumes of ion conducting glasses. In the case of our experimental setup, the size of the subvolume was about $(40\ \mathrm{nm})^3$. Thus, the technique should be very powerful for characterizing nano- or mesoscale structured solid electrolytes.

In this paper, we report on the application of TD-EFS to a $LiAlSiO_4$ glass ceramic with 42% crystallinity. At this degree

of crystallinity, the lithium ion conductivity becomes maximal [6]. According to Ref. [13], the average size of the crystallites in this glass ceramic is about 300 nm. Since the ionic conductivity of the crystallites is much lower than that of the glassy phase [6], this glass ceramic is an interesting model material for obtaining a better understanding of ion transport in nano- and mesoscale structured solid electrolytes. The most important result of our TD-EFS measurements is that we can distinguish two dynamic processes, while only the faster of these two processes is observable in the macroscopic conductivity spectra of the glass ceramic.

2. Experimental

For the experiments we use a commercial, variable-temperature AFM operating under ultrahigh vacuum (UHV) conditions (Omicron VT-AFM). The sample temperature can be varied in the range from 30 K up to 650 K. The force sensor is a single crystalline, highly doped silicon cantilever with a resonant frequency of 300 kHz and a spring constant of 20 N/m, featuring a sharp conducting tip with an apex radius of 10 nm (non-contact cantilever of type NCHR from Nanosensors). The system is operated in the frequency modulation-mode (FM-mode) [14], where the cantilever is always oscillating at the resonant frequency. Conservative tip-sample forces will induce a shift in the resonant frequency, which is used as the feedback parameter for the tip-sample distance control during surface scanning.

During the TD-EFS experiments, we measure the electrostatic forces between a sample which is kept at ground potential, and a conductive tip which is biased with a voltage of -2 V. The electric field emanating from the tip penetrates into the sample over a distance comparable to the tip diameter [15]. Detailed finite element simulations using the FEMLAB software yield an approximate probed sample volume of $(40\ \mathrm{nm})^3$ [12]. If the tip bias is negative, positively charged ions will be attracted towards the region penetrated by the electric field. Therefore, the probed sample volume will charge up positively compared to the surrounding region. This leads to an increase of the electrostatic force felt by the tip and causes a negative frequency shift. The accumulation of charged ions will continue until an equilibrium is reached. Thus, the time-dependent change of the frequency shift is a direct fingerprint of the dynamic conductance behaviour of the ions.

In Fig. 1 we sketch the basic idea behind our TD-EFS measurements on a partially crystallised glass ceramic. Depending on the position of the tip, the probed sample volume contains different amounts of glassy and crystalline phases. Since the ionic conductivity in these phases is different, we expect the electrostatic force spectra to depend on the position of the tip.

For the preparation of a glass ceramic with 42% crystallinity we first prepared a glass sample as described in Ref. [6]. The surface roughness of this sample was reduced to about 1-2 nm by using the polishing techniques described in Ref. [12]. Subsequently, the sample was annealed in order to generate partial crystallisation [6]. The surfaces of the resulting glass ceramic was either left untreated or lightly polished with a water-free 1/4 micron diamond suspension by means of a Q-tip.

The TD-EFS measurements were carried out in a temperature range from 295 K to 607 K. The main complication during these measurements is temperature–induced drift of the tip-sample distance, especially at elevated temperatures. To account for this effect, we first measure the drift of the sample over a period of some minutes. The drift rate is then calculated and during the following spectroscopic measurements the tip position is corrected for this drift rate.

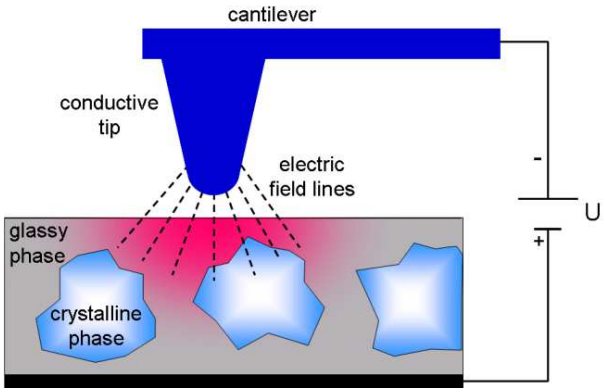


FIG. 1: Schematic illustration of the experimental setup for time-domain electrostatic force spectroscopy (TD-EFS) on a partially crystallised glass ceramic.

3. Results

Before carrying out the TD-EFS measurements we first scanned a small area of the sample surface. Fig. 2 shows a typical 400 400 nm scan. We observe protrusions on the surface with a typical diameter of 50 to 100 nm and a height varying between 5 and 15 nm. It is not clear at this point if these protrusion can be interpreted as crystallites which grow out of the surface.

For each sample temperature we performed spectroscopic measurements at different positions of the tip above the surface, following the procedure decribed above. As an example Fig. 3 shows the frequency shift of the oscillating cantilever as a function of time, for $T = 506\,\mathrm{K}$, at five different positions, indicated by the circled numbers in Fig. 2. To start the spectroscopy measurement the distance feedback is disabled and the tip is retracted by 1 nm. At time $t = 0$ sec, a voltage of $U =$ 2 V is applied to the tip. The relaxation curves show a sudden large negative frequency shift Δf_{fast} due to fast relaxation processes. Subsequently, slow relaxation processes are monitored until the system has reached its saturation frequency value $\Delta f_{\mathrm{fast}} + \Delta f_{\mathrm{slow}}$. The slow relaxation process can be fitted with a stretched exponential function [16]:

$$\Delta f(t) = (\Delta f_{\mathrm{slow}} \quad \Delta f_{\mathrm{fast}}) \quad \left[1 \quad \exp\left(-(t/\tau)^{\beta}\right)\right] + \Delta f_{\mathrm{fast}} \tag{1}$$

where τ and β denote the temperature-dependent relaxation time and the stretching exponent, respectively.

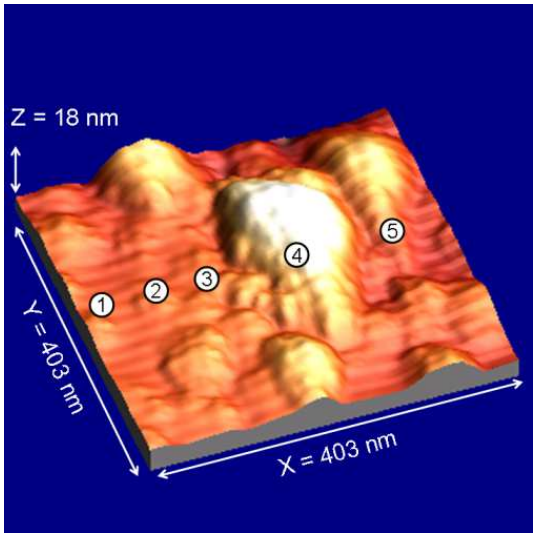


FIG. 2: Surface topography of the partially crystallised glass ceramic. The circled numbers denote tip positions during the recording of the TD-EFS relaxation curves shown in Fig. 3.

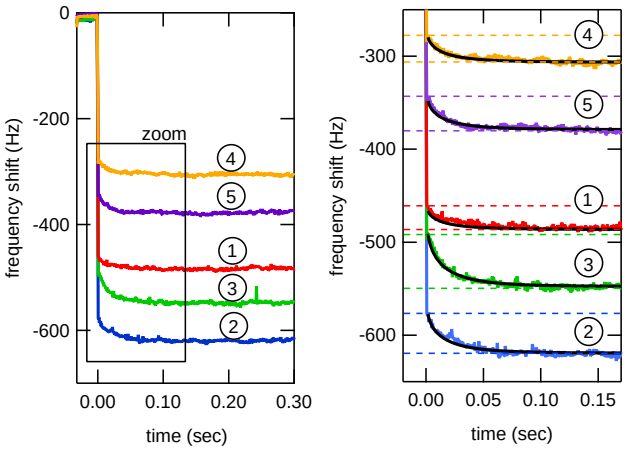


FIG. 3: TD-EFS relaxation curves at a temperature of T = 506 K, obtained at the positions indicated by the circled numbers in Fig. 2.

For the interpretation of the relaxation curves one has to take into account that the investigated solid electrolyte consists of crystallites embedded in a glassy matrix. From macroscopic conductivity measurements [6] it is known that $LiAlSiO_4$ glass is a moderate ion conductor with an activation energy of $E_A^{\mathrm{glass}} = 0.72$ eV, while a completely crystallised $LiAlSiO_4$ sample is a poor ion conductor with a high activation energy of $E_A^{\mathrm{crystal}} = 1.07$ eV. At room temperature, the macroscopic electrical relaxation times $\tau_{\mathrm{macro}} = R_{\mathrm{macro}} C_{\mathrm{macro}}$ [12] of the pure glass and of the completely crystallised ceramic are about 10^{-2} s and 10^{3} s, respectively. Here, R_{macro} und C_{macro} denote the macroscopic resistance and capacitance, respectively.

This suggests that at room temperature, the TD-EFS relaxation curves of the glass ceramic are determined by movements of ions in the glassy phase and possibly at the glass-crystal interfaces [6], while the ions in the crystallites do *not* contribute to the relaxation. This implies that $\Delta f_{\mathrm{slow}} = \Delta f_{\mathrm{glass}} + \Delta f_{\mathrm{interfaces}}$. The offset Δf_{fast} is due to ultrafast vibrational and electronic polarisations. In an Arrhenius plot in Fig. 4 the relaxation times due to ionic movements are shown as blue squares. A fit with an Arrhenius equation (dashed blue line) yields an activation energy of (0.62 0.1) eV. For comparison, the solid blue line denotes the macroscopic electrical relaxation time with an activation energy of 0.72 eV. Within the experimental error, the TD-EFS and the macroscopic relaxation times are similar. However, the TD-EFS relaxation times are characterised by a higher preexponential factor.

At temperatures above 420 K, the relaxation process becomes so fast that it cannot be distinguished anymore from the ultrafast vibrational and electronic polarisation. At temperatures above 500 K, we detect an additional slower relaxation process with an activation energy of (1.11 0.07) eV, see red crosses (data) and dashed red line (fit) in Fig. 4. Representative relaxation curves at a temperature of T = 506 K are shown in Fig. 3. The solid black lines represent stretched exponential fits for the determination of the relaxation times τ. Although the values of Δf_{fast} and Δf_{slow} vary considerably for the different positions on the surface, the relaxation times are consistent for the different curves. Remarkably, the activation energy of the slow relaxation process is almost identical to the activation energy for the macroscopic electrical relaxation times of a completely crystallised $LiAlSiO_4$ ceramic. These macroscopic relaxation times are denoted by the solid red line in Fig. 4, corresponding to an activation energy of 1.07 eV.

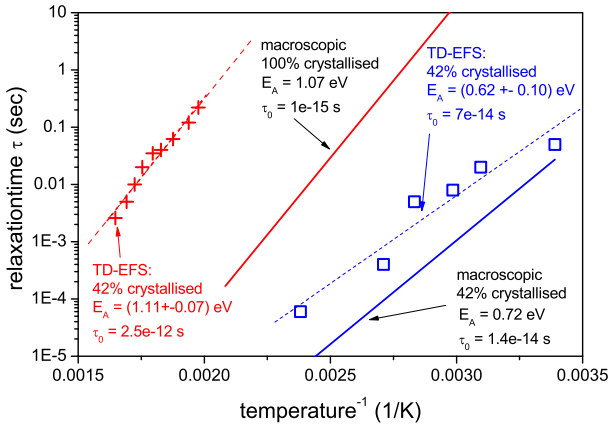


FIG. 4: Arrhenius plot of TD-EFS relaxation times (symbols) and macroscopic relaxation times (solid lines) obtained for a glass ceramic with 42% crystallinity and for a completely crystallised ceramic. The dashed lines denote Arrhenius fits of the TD-EFS relaxation times.

4. Discussion

Our results cleary demonstrate that macroscopic averaging over the dynamics of all ions in the glass ceramic leads to a considerable loss of information. The macroscopic dc conductivity is determined by the long-range ion transport along percolative diffusion pathways. Such percolative pathways exist in the glassy phase and along the glass–crystal interfaces [6]. In comparison, the lithium ions in the crystallites move much slower, and the crystallites do not form a percolative network [6]. Therefore, the slow movements of the ions in the crystallites do not contribute significantly to the macroscopic dc conductivity. However, when we use TD-EFS as a local probe, we detect two distinct relaxation processes. The activation energy of the faster process is, within the experimental error, similar to the activation energy of the macroscopic dc conductivity. This suggests that this process is due to ionic movements in the glassy phase and at the glass–crystal interfaces. The activation energy of the slower process is similar to the activation energy for macroscopic ionic conduction in a *completely crystallised* ceramic. This indicates that the slow process we detect in our TD-EFS measurements on the *partially crystallised* glass ceramic is due to ionic movements in the crystallites. Since the crystallites do not form a percolative network, the ionic movements are localised and do not lead to a long-range ionic diffusion. While such localised motions do not contribute to the macroscopic dc conductivity, they contribute potentially to the macroscopic ac conductivity. However, in the macroscopic ac conductivity spectra of the glass ceramic with 42% crystallinity, a process with an activation energy of about 1.1 eV is not detectable. This can be explained by the large ac conductivity contribution of the fast ions in the glassy phase and at the glass-crystal interfaces, which buries the ac conductivity contribution of the slow ions in the crystallites. In contrast, by means of TD-EFS, the slow process is detectable, when the probed sample volume is filled to a large extent by crystallites.

An interesting question concerns the physical origin of the discrepancies between the preexponential factors of the macroscopic and of the TD-EFS relaxation times. In the case of the fast process, the preexponential factor of the TD-EFS relaxation times is slightly higher than the preexponential factor of the macroscopic relaxation times. One possible reason lies in the influence of the vacuum capacitance, due to the gap between tip and sample, on the TD-EFS relaxation times, which complicates a quantitative comparision between macroscopic and TD-EFS relaxation times [12]. In the case of the slow processes, we find that the preexponential factors of the relaxation times differ by about three orders of magnitude. However, here we have to take into account that the macroscopic and the TD-EFS measurements probe different processes. The macroscopic conductivity spectra of the completely crystallised glass ceramic are governed by long-range ionic diffusion in a percolating network of crystallites. The TD-EFS relaxation times of the glass ceramic with 42% crystallinity are determined by local movements of ions in isolated crystallites. While the activation energies of these distinct processes seem to be similar, it is plausible that their preexponential factors differ considerably.

In Fig. 3 we have shown that the relaxation strengths of both the fast and the slow relaxation process depend strongly on the position of the tip. This result can be easily understood, since the relative amounts of glassy phase and crystallites in the probed subvolume change when the tip moves to a different position. A large amount of glassy phase leads to a high relaxation strength of the faster relaxation process, while a large amounts of crystalline phase leads to a high relaxation strength of the slower relaxation process. Therefore, our method potentially allows us to obtain spatially resolved spectroscopic data and to create images of the relative contributions of the different processes. Such images should provide comprehensive information about the size and the distribution of the crystallites in glass ceramics. This will be the subject of future work.

5. Conclusions

We have shown that TD-EFS measurements provide information about ionic movements in a partially crystallised glass ceramic, which is beyond the information obtainable by macroscopic electrical spectroscopy. By means of TD-EFS, we have detected two distinct relaxation processes with different activation energies. The faster process is characterised by an activation energy similar to the activation of the macroscopic electrical conductivity. Our results indicate that this relaxation process is due to ionic movements in the glassy phase and at the glass–crystal interfaces. The slower process detected by TD-EFS does not contribute to the macroscopic electrical conductivity of the glass ceramic. The activation of this process is, however, similar to the activation energy for ionic conduction in a *completely* crystallised $LiAlSiO_4$ ceramic. This suggests that the slow relaxation process in the partially crystallised glass ceramic is caused by localised ionic movements in isolated crystallites.

The relaxation strengths of the two processes depend on the position of the AFM tip above the surface. This reflects the spatially varying amounts of glassy phase and crystalline phase being present in the probed subvolumes of the sample, when the tip is moved between different positions. Thus, the TD-EFS method can be used to obtain information on size and distribution of the crystallites in the glassy matrix, i.e. information on the nano- and mesoscale structure of the material.

Acknowledgements

We would like to thank the Deutsche Forschungsgemeinschaft and the Fonds der Chemischen Industrie for financial support of this work.

Based on a talk given at the 84th International Bunsen Discussion Meeting on the 'Structure and Dynamics of Disordered Ionic Materials' (Münster, Germany, October 6-8, 2004).

[1] W. Pannhorst, *J. Non-Cryst. Solids* **219** (1997) 198–204.
[2] W. Pannhorst, *Glass Technol.* **45** (2004) 51–53.
[3] O. Shilova, *Glass Technol.* **45** (2004) 59–61.
[4] Y. Zhang, J. D. Santos, *J. Non-Cryst. Solids* **272** (2000) 14–21.
[5] W. Höland, V. Rheinberger, M. Schweiger, *Phil. Trans. R. Soc. London* **361** (2003) 575–589.
[6] B. Roling, S. Murugavel, *Z. Phys. Chem.* (2004), in press.
[7] S. Indris, P. Heitjans, H. E. Roman, A. Bunde, *Phys. Rev. Lett.* **84** (2000) 2889–2892.
[8] F. Croce, G. B. Appetecci, L. Persi, B. Scrosati, *Nature* **394** (1998) 456–458.
[9] F. Croce, R. Curini, A. Martinelli, L. Persi, F. Ronci, B. Scrosati, *J. Phys. Chem. B* **103** (1999) 10632–10638.
[10] B. Scrosati, F. Croce, L. Persi, *J. Electrochem. Soc.* **147** (2000) 1718–1721.
[11] J. Maier, *Prog. Solid St. Chem.* **23** (1995) 171–263.
[12] A. Schirmeisen, A. Taskiran, H. Fuchs, B. Roling, S. Murugavel, H. Bracht, F. Natrup, *Appl. Phys. Lett.* **85** (2004) 2053–2055.
[13] R. M. Biefeld, G. E. Pike, R. T. Johnson Jr., *Phys. Rev. B* **15** (1977) 5912–5920.
[14] T. R. Albrecht, P. Grütter, D. Horne, D. Rugar, *J. Appl. Phys.* **69** (1991) 668–673.
[15] S. Gomez-Monivas, L. S. Froufe-Perez, A. J. Caamano, J. J. Saenz, *Appl. Phys. Lett.* **79** (2001) 4048–4050.
[16] L. E. Walther, N. E. Israeloff, E. Vidal Russel, H. Alvarez Gomariz, *Phys. Rev. B* **57** (1998) R15112–R15115.